Universiteit Leiden
The Netherlands

**Opleiding Informatica en Economie**

# Improvements to an existing, ultrasound localization system, enhancing communication robustness

Stan van der Plas

Supervisors:

Richard van Dijk & Mitra Baratchi

BACHELOR THESIS

Leiden Institute of Advanced Computer Science (LIACS)

www.liacs.leidenuniv.nl 29/08/2024

**Abstract**

This thesis describes extensions and improvements of an ultrasound-based indoor localization system developed by students at LIACS, Leiden University. The goal of these improvements is to enhance the system's reliability and robustness in maintaining accurate communication between the tracking devices and the objects being tracked. We investigated the accuracy of the HC-SR04 Ultrasonic Distance Sensor used in the system, in the direct method architecture and evaluated its performance against the traditional reflective method. Secondly, we measured the thickness of objects passing between the sensors, which could help maintain accuracy among distance measurements even when the line of sight is interrupted. Thirdly, we examined how to preserve sensor accuracy and time-resolution when trigger signals are sent sequentially rather than simultaneously; a common challenge in ultrasound localization systems.

Fourthly, we automate the setup of the beacons without manual distance measurements to improve the system deployment speed and reduce chance for human error. Fively, we analyzed the performance of the developed ultrasound system for tracking a moving object, focusing on both accuracy and the reliability of the received signals. And finally, a method for determining the orientation of the tracked object was developed.

# Contents

To aid the reader's understanding, the following table defines key terms and concepts used throughout this thesis:

| **Term** | **Definition** |
|---|---|
| Ultrasound Sensor | A device that uses high-frequency sound waves to measure distances by calculating the time of flight. |
| Beacon | A stationary device that emits a signal to be received by the tag. |
| Tag | A movable device that receives signals from beacons and whose position is tracked. |
| RTLS (Real-Time Localization System) | A system that provides location information in real-time. |
| UWB (Ultra-Wideband) | A radio technology that uses a wide frequency spectrum to achieve high precision in distance measurement. |
| Line of Sight | A direct path between the sensor and the object being measured, without obstruction. |
| Direct Method | A technique where measurements are taken directly between the sensor and the object without reflective surfaces. |
| Reflective Method | A technique where measurements are based on the reflection of signals from surfaces or objects. |
| Trigger signal | Signal sent from the microprocessor to the sensor to initiate a distance measurement |

Table 1: Table of Terms and Definitions

# 1 Introduction

Accurate indoor localization systems are increasingly important in various domains such as healthcare, logistics, and robotics. These systems are used for tracking objects, navigating autonomous vehicles, and improving operational efficiency within confined spaces like warehouses and hospitals. While positioning systems such as the Global Positioning System (GPS), provide reliable location data, their signals cannot penetrate walls or roofs effectively, rendering them unusable indoors. As a result, Indoor Positioning Systems (IPS) have been developed using a wide range of technologies. These technologies including Bluetooth, Wi-Fi, Ultra-Wideband (UWB), and many others as illustrated in Figure 1, which highlights the broad spectrum of technologies that have been employed for both indoor and outdoor localization.

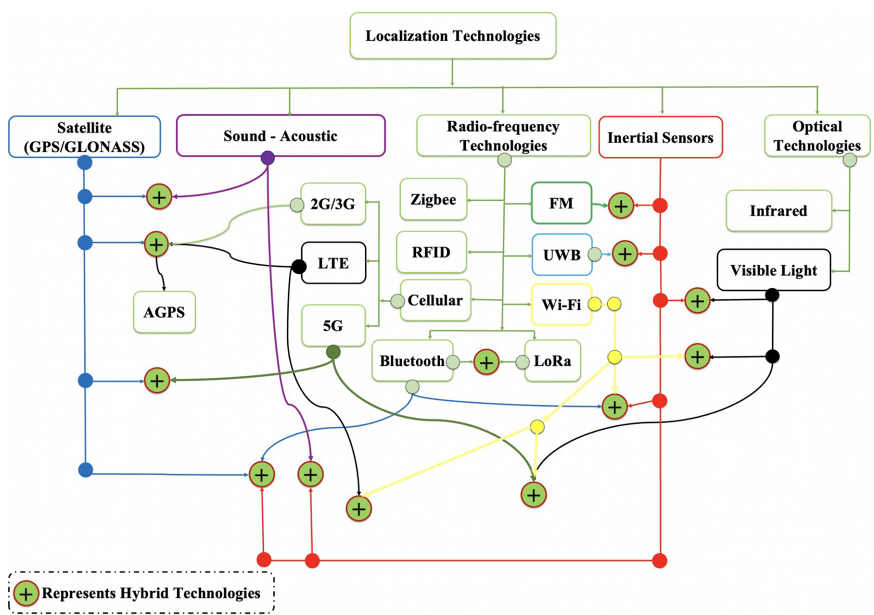


Figure 1: Technologies used for localization [AM22]

Among the technologies explored for indoor localization, Ultrasound-based Indoor Positioning Systems (UIPS) stand out due to their potential for high accuracy and relatively low cost. However, UIPS also present challenges, such as dependency on line-of-sight and signal interference. These factors limit the practicality of ultrasound systems, especially in dynamic environments where objects or people move unpredictably. Previous systems, like the one developed by Bas van Aalst [vA23] at LIACS, Leiden University, used ultrasound to track objects, but required objects to face the sensors for accurate tracking, reducing usability. Additionally, manually measuring the placement of the sensors during the setup of the system made deployment time-consuming and prone to errors.

This thesis aims to refine and improve the existing ultrasound-based system by addressing its key limitations. Specifically, the goal is to develop a UIPS that employs the direct method, where ultrasound sensors are positioned to measure signals from the sensor directly facing them. This method, as demonstrated in Bas van Aalst's research, has shown significant promise in achieving high accuracy. Automating the calibration will also be researched to improve the speed of deployment, reduce manual errors, and enhance the system's overall usability. The system will also support orientation determination of the tracked objects, a functionality not present in many existing UIPS. To achieve this, the research will tackle several challenges, including managing line-of-sight interruptions and developing a novel timing synchronization method that does not require additional types of sensors.

By improving the robustness, flexibility, and ease of deployment of the UIPS, this thesis aims to offer a cost-effective alternative to existing UWB systems. UWB-based systems, such as those developed by Pozyx, provide high accuracy but come with high costs. The proposed ultrasound system, by contrast, seeks to deliver comparable performance in terms of accuracy while maintaining a simple, budget-friendly design.

## 1.1 Objectives

The primary objective of this thesis is to develop an UIPS that utilizes the direct method. The system should have high accuracy and the necessary functionalities, namely orientation determination and automated calibration. To achieve these objectives, the research will address several challenges: evaluating the accuracy of the direct method, managing interruptions in line of sight for reliable localization, and developing a novel timing synchronization method that eliminates the need for additional sensor types. The UIPS will be assessed to determine whether it can effectively replace existing UWB-based systems in terms of accuracy and functionality.

## 1.2 Research questions (RQ's)

The main research question is how to make the current ultrasound system more mature in terms of automated setup and calibration, correction of localization in severe conditions, improved accuracy and time-resolution, measuring the orientation of the object, and comparison with an RTLS based on UWB sensors. This question is subdivided into the following six sub-research questions:

RQ1:
*What is the accuracy of the HC-SR04 Ultrasonic Distance Sensor when using the direct method*
HC-SR04 ultrasound distance sensor is not used in the intended architecture designed by the producer, which is referred to as the reflective method in this thesis. We like to measure and improve the localization accuracy of the chosen architecture, using the direct method.

RQ2:
*Is it possible to localize objects if another object passes through the line of sight by measuring the thickness of this object?*
If the thickness of an object passing through the line of sight is measurable, than it can be used to calculate the distance between the tag and the beacon, even when the line of sight is interrupted.

RQ3:
*How can accuracy of the sensors be maintained if the trigger signals aren't sent at the same moment?*
The sensors will be connected to hardware with multiple physically separated processors, where the trigger signals are send sequentially. This must be corrected for the calculation of the distance.

RQ4:
*Can beacons be set up in any position without manual distance measure?*
This automated deployment of the system, also present in the UWB system of Pozyx, will improve the speed and error sensitivity of the system setup.

RQ5:
*Can ultrasonic sensors effectively replace UWB sensors in object tracking?*
The answer to this question will determine whether the objective has been fulfilled.

RQ6:
*Is it possible to determine the orientation of the tag from sensor connections to beacons?*
This is another functionality that is present in the UWB system and increases the usability of the system.

## 1.3 Background

### 1.3.1 Ultrasound Sensors

Ultrasound sensors are devices that can send and receive ultrasound waves. One of the most useful attributes of these sensors is their ability to measure the time it takes for a signal to travel from the sender to the receiver [Unk1]. The time-of-flight of the signal can then be used to calculate the distance with sub-millimeter accuracy, some methods of setting up the sensors have been implemented in this research [Ali22]. These sensors are commonly used in cars for parking assistance, where they can alert the driver if an object gets too close while parking [AMTF+11]. Many ultrasound sensors emit sound waves that travel through air, known as air-coupled transducers. There are also contact transducers, which have direct contact with the object they are measuring which are often used for medical imaging, commonly known as ultrasound scans [OCVM21]. Ultrasound scans create an image of the inside of the body using many small contact transducers [MKKB10].

### 1.3.2 Sound propagation and reflection

Sound travels through the air as a wave of pressure changes caused by vibrating particles. The speed of sound varies with the medium and depends on its elastic and inertial properties. Sound travels faster in less compressible, denser media and the temperature also influences the speed significantly [Ope16a], the useful formulas are depicted in Figure 2.

As sound waves travel further, they attenuate, losing energy and becoming weaker. When sound waves encounter a different medium, part of the sound is reflected back while the rest is transmitted into the new medium [Ope16b]. The direction of the reflected sound depends on the angle at which it hits the boundary, following Snellius' law: the angle of incidence equals the angle of reflection. The fraction of sound that is reflected back is determined by the acoustic impedance of the two media, which is a measure of how much resistance the medium provides to the sound wave [MKKB10]. This foundation informs our practical testing, which identifies materials that effectively reflect sound back to the sensor.

General

$$v = \sqrt{\frac{\text{elastic property}}{\text{inertial property}}}$$

Ideal Gas

$$v = \sqrt{\frac{\gamma R T_K}{M}}$$

Air at sea level

$$v = 331\ m/s \sqrt{1 + \frac{T_C}{273^{\circ} C}}$$

Figure 2: Speed of sound formulas

## 1.4 Thesis overview

The relevant academic work related to this thesis in described in Section 2 which is useful for understanding the foundations of the proposed system. Section 3 explains the method of how this thesis intends to answer the research questions. Each research question is described in a separate chapter. The experiments that are done to facilitate the answering of research questions are formulated in Section 4. The results of the experiments are shown in Section 5. These results are analyzed and used for conclusions that will be drawn in Section 6, along with future research that could further improve the ultrasound system.

# 2 Related Work

## 2.1 Real Time Localization systems

Real Time Localization systems (RTLS) are technologies that are used to determine the position of an object or person within a certain space. One of the most widely known and used localization systems is the Global Positioning System (GPS). GPS uses a network of satellites that transmit signals to a receiver. By measuring the time it takes for these signals to travel the system can calculate the receiver's exact position through triangulation. Triangulation uses the distances from at least three known points to the unknown point to calculate its location, this formula is used in our system.

While GPS is highly effective outdoors, its signals cannot penetrate walls, rendering it unsuitable for indoor environments. As a result, various indoor localization systems have been developed to provide accurate positioning within buildings. These systems rely on one or more of the following technologies and methods: AGPS, 2G/3G, LTE, 5G, Zigbee, RFID, cellular networks, Bluetooth, FM, UWB, Wi-Fi, LoRa, infrared, visible light, and sound [AM22]. To keep costs low, these systems often utilize existing devices, such as smartphones or smartwatches, which can use many of these technologies [TKL12] [SNM20].

Ultra-wideband (UWB) is a promising technology for indoor localization because of its high precision. UWB systems transmit signals over a wide frequency spectrum, allowing for precise time-of-flight measurements [SS18]. UWB is capable of high data rates, has low power consumption, and the capability to support multiple devices and networks simultaneously. Pozyx [1] is a company that creates UWB systems that are accurate enough so that research can be conducted using the system measurements, which is sometimes used as a benchmark to compare our system to [MMES+20].

## 2.2 Ultrasound localization systems

Ultrasound-based indoor positioning systems (UIPS) provide a promising alternative to more expensive technologies like UWB. These systems often use

[1]Information about their system can be found at: `https://www.pozyx.io/nl`.

trilateration, similar to GPS, to calculate positions based on the time-of-flight of ultrasound signals. Bas van Aalst [vA23] developed an early ultrasound-based indoor positioning system using this trilateration approach, which this research continues to build upon by refining its core methodology. His system relies on a direct communication method between a pair of ultrasound sensors. This direct method allows the system to use a simpler design compared to most UIPS, but it has not been widely explored in existing literature, which makes it a unique focus of this research.

A significant challenge for ultrasound systems is timing synchronization. Accurate time-of-flight measurements require precise timing. While GPS systems use atomic clocks, this isn't feasible for larger systems tracking many devices [BW99]. Zero Key has developed a system that uses a hybrid of ultrasound and UWB to tackle these timing problems. The system can achieve high accuracy on distances greater than 10 meters, with individual measurements accurate to approximately 2mm and an average error of less than 1mm after applying a Kalman filter [DDM20]. Similarly, a research uses ultrasound for distance estimation, RF signals for timing synchronization, and Wi-Fi for communication to ensure high precision and robust performance [QL17].

However, this research distinguishes itself by aiming to simplify the localization process and reduce system complexity. Instead of relying on hybrid systems, it focuses solely on ultrasound for both communication and measurement. Other approaches have used ultrasound alone for accurate localization, combining methods such as wideband spread spectrum signaling with angle of arrival (AoA) and time of flight (ToF) [SBBD12]. This research refines the direct two-way communication method to overcome challenges such as signal interference and timing synchronization. While some systems address these issues by combining different sensor types, this research investigates how ultrasound alone can maintain high accuracy by drawing from best practices in both real-time localization systems (RTLS) and existing UIPS literature.

# 3 Methods

## 3.1 Materials used

### HC-SR04 ultrasonic distance sensors

The HC-SR04 sensors are the only sensors that will be used in this research. They are selected for their cost-effectiveness, detailed user manual and high accuracy. These are the specifications listed in the HC-SR04 user's manual [Unk1].

The sensors are air-coupled transducers that send out ultrasound signals

Table 2: specifications

| Parameter | Value |
|---|---|
| Operating Voltage | 3.3Vdc $\sim$ 5Vdc |
| Operating Frequency | 40KHz |
| Operating Range | 2cm $\sim$ 400cm |
| Accuracy | $\pm$ 3mm |
| Sensitivity | $-65$dB min |
| Sound Pressure | 112dB |
| Effective Angle | 15° |
| Connector | 4-pins header with 2.54mm pitch |
| Dimension | 45mm x 20mm x 15mm |

through the air. After triggering the sensor, it initiates measurements by emitting an 8-cycle burst of ultrasound. The echo pin is raised after the burst is sent out. Once the sensor detects the echo of the ultrasound, the echo pin is lowered. The duration for which the echo pin remains raised corresponds to the time interval between the transmission of the trigger signal and the reception of the echo signal. This interval is the data send to the microprocessor.

### Arduino

To control the sensors, a controller board is needed. Since the proposed system requires minimal processing power, we have chosen the Arduino UNO R3. This controller board was selected for its low cost, compact size, and extensive library support, which makes it easy and fast to develop the necessary code to control the sensors.

### Laptop

The Arduino is connected to a laptop to upload the correct programs and store the measurement data.

### Connecting hardware

For the system to operate, various components need to be connected, specifically linking the computer to the Arduinos and the sensors to the Arduinos. A schematic overview of how most of the hardware is connected is shown in Figure 3. The following items were used to achieve these connections:

1. **USB Hub**
   - **Purpose**: Allows multiple USB devices to connect to a single USB port on the computer.
   - **Details**: A USB hub with 7 ports was used to accommodate the connection of multiple Arduinos to the computer.
2. **USB Cables**
   - **Purpose**: Connect the Arduinos to the computer for both power and data transfer.
   - **Details**: 5-meter-long USB cables were chosen to allow the Arduinos to be placed at a distance from the computer, providing flexibility in setup.
3. **Breadboards**
   - **Purpose**: Facilitate the easy connection and reconfiguration of the sensors and Arduinos.
   - **Details**: Breadboards provide a convenient platform for connecting the sensors to the Arduinos without soldering.
4. **Breadboard Jumper Wires**

- **Purpose**: Establish connections between the breadboards and the Arduinos.
- **Details**: 30-centimeter male-to-male jumper wires were used to connect the sensors on the breadboards to the input/output pins of the Arduinos.

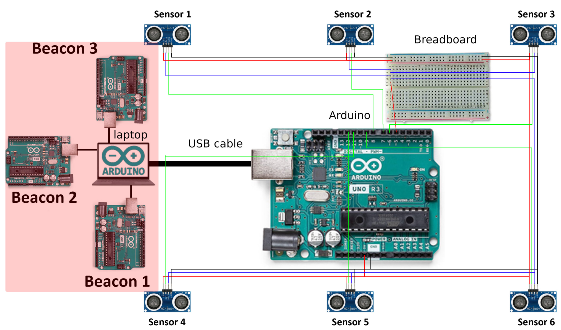


Figure 3: 4 Arduino's connected to a laptop, 6 sensors to 1 Arduino

### Tag

The moving object that is tracked, referred to as the tag, must contain at least one ultrasound sensor. This tag, however, is equipped with six sensors and designed in the shape shown in Figure 16 to facilitate the determination of its orientation, as will be explained later in Section 3.6. The tag was specifically designed and 3D printed to meet the spatial arrangement and functional requirements necessary for this system.

### Tripods

Tripods are used to place the beacons, or anchors, in specific setups. This allows for easy and accurate deployment of the setups for testing.

### Train

A toy train is used to provide an object with constant and predictable movement for testing. The train supports the weight of the tag but exhibits

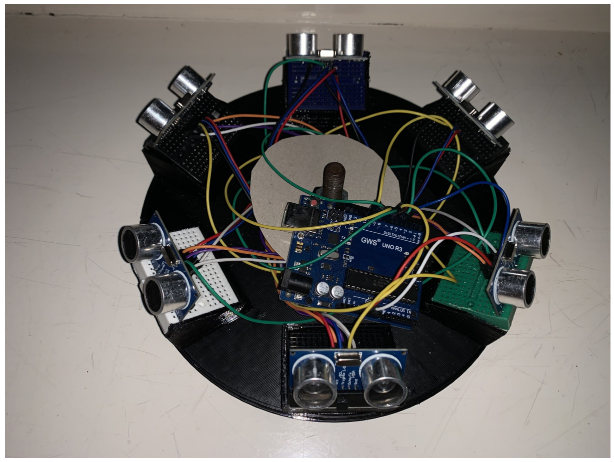

Figure 4: Tag with connected sensors

noticeable wobbling. However, this wobbling is unlikely to significantly affect the results.

**Office objects**

Various common office objects were used to test the reflective properties in the setup. These objects include aluminum foil, a sock, a tennis ball, an apple, a tape holder, a fuzzy hat, and a notebook.

## 3.2 RQ1: Accuracy of the direct method

For this research, the sensors used are HC-SR04 ultrasonic distance sensors. The reason for this sensor choice is the low price and high accuracy. Typical use of these sensors is with the reflective method. However, there are situations in which this method of measuring is unreliable. For example, there might be people walking in the operating area of the sensor. This would cause the sensor to measure the distance to the person instead of measuring to the intended object. This characteristic makes the sensor unreliable in situations where multiple objects are present in it's line of sight. This limitation, combined with the fact that not all surfaces reliably reflect sound back to the sensor, makes the reflective method unsuitable for the localization system in this thesis.

### 3.2.1 Reflective method

The reflective method works on the principle that sound is reflected by an object, as shown in Figure 6. The time difference between sending and receiving the signal is used to calculate the distance between the sensor and the object, the calculation is shown in Equation 1. In this calculation, the speed of sound is used to determine the distance. The information given in the Sensor Module User Guide is that the operating range is 2-400 cm with an accuracy of ±3mm [Unk1]. The angle at which the sensor can effectively measure is up to 15 degrees from the center line. This effective operating angle means that a person, as described in the example, does not have to block the line of sight between the sensor and an object to interfere with the measurement. If the person is closer to the sensor and within the operating range, the sound reflected from the person will reach the sensor before the sound reflected from the object. Since the sensor stops measuring as soon as the first reflection is received, it will always measure the distance to the closest object in its path. That leads to the sensor not measuring the intended distance.

$$\begin{aligned}\text{Distance measured} &= \text{Time measured} \times \text{Speed of sound} \\ &= (\text{Time signal received} - \text{Time signal triggered}) \times \text{Speed of sound}\end{aligned} \tag{1}$$

Figure 5: Distance measurement sensor

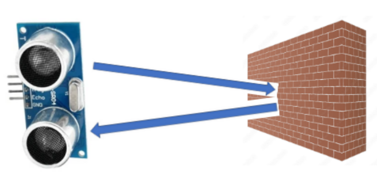

Figure 6: Reflective method

### 3.2.2 Direct method

The direct method used in this thesis, visualized in Figure 7, operates on a different principle compared to the reflective method. This method uses two sensors facing each other, each sensor sending a signal that is received by the other. Since each sensor can effectively measure up to 15 degrees from its center line, the combined field of view extends to a total of 30 degrees from the center line, offering a broader detection area. Bas van Aalst conducted a test to determine the range of the field of view [vA23]. He did not provide a specific numerical value, but the figure he presented suggests that the total field of view is about 60 degrees, which aligns with our assumption of 30 degrees from the center line.

Using two sensors provides a higher level of certainty in the measurement process. When both sensors measure the same distance, this confirms that the measurement process is accurate. The sound travels the same distance in both directions and should take the same amount of time to reach the opposite sensor. This symmetry ensures the reliability of the measurements. If there is a discrepancy between the measured distances, it signals potential issues in the measurement process. This built-in error detection feature is not present in the reflective method, making the direct method more reliable.

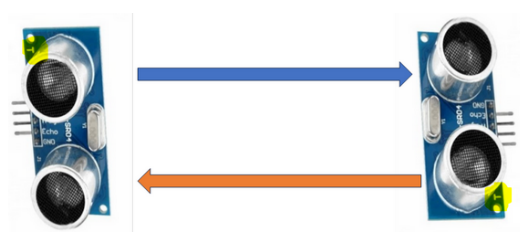

Figure 7: Direct method

### 3.2.3 Accuracy of the direct method

The direct method uses sensors in a non-standard configuration, so we cannot assume they maintain the same accuracy as in the reflective method. To evaluate the accuracy of the sensors in the direct setup, we follow the research of Fuad Aliew as a guideline [Ali22]. Aliew tested the accuracy of ultrasound sensors in the reflective method and identified conditions for optimal measurements, such as the absence of nearby objects that could reflect sound waves and the need for constant temperature monitoring. While temperature affects the speed of sound (2), our testing indicated that sub-millimeter accuracy was not achievable in our setup. Given that temperature variations within a typical indoor range (e.g., 17 to 22 degrees Celsius) result in less than a 1% change in the speed of sound, we concluded that adjusting for this would not significantly improve accuracy. Therefore, only one temperature was used for the entire test [PN11]. In our setup, the reflective surface is replaced with a second sensor.

Aliew does not specify the exact sensor model used in his study, but several factors suggest that it may be the same as the HC-SR04 sensor we are using. First, both sensors are low-cost. Second, they operate at 40kHz and utilize an 8-cycle burst of ultrasound. Third, Aliew's research shows an accuracy range of 1 to 8 mm, where 1 mm is better than the sensor's specified accuracy and 8 mm is worse. This range is consistent with our sensor's stated accuracy of 3 mm (see Table 2). Given these similarities, it is likely that the sensors used in both studies are the same model.

Aliew's method for determining sensor accuracy is extensive, involving measurements taken at each centimeter [Ali22]. His research mentions that measurements follow a Gaussian distribution, where increasing the number of measurements improves accuracy. However, after approximately 100 measurements, the benefits diminish due to the impracticality of additional measurements over time. Aliew tested several methods to improve accuracy, including the least-squares method, the Vandermonde method, and his smart filter, with the smart filter achieving the best results, reaching sub-1 millimeter accuracy. Unfortunately, the specifics of the smart filter are not provided in Aliew's paper, so we cannot apply this method to our setup.

In our study, practical constraints limited testing to four different distances, each measured with multiple sensor combinations over 60-second intervals, producing well over 100 measurements.

Zero Key's commercially available UIPS uses a Kalman filter to go from an individual measurement error of approximately 2mm to an average error of sub-1 millimeter. This improvement shows that advanced filtering techniques can significantly increase accuracy regardless of what ultrasonic sensor is used [DDM20]. Many other methods like the Kalman filter have been developed to improve the accuracy of ultrasound sensors. While integration of these advanced techniques could potentially enhance tag position estimation, it falls outside the scope of this thesis, which concentrates on implementing the direct method rather than identifying optimal data filtering methodologies.

To determine accuracy, we will use the conventional approach of comparing the average measurements over time to the actual distance. These measurements will be made while the sensors are not moving, at distances from 20 to 200 centimeters. The consistency of the measurements will also be determined since that is a relevant aspect of accuracy. To confirm the accuracy of the distance measured, we also included multiple different sensors. This is required since each sensor might behave differently which was possibly observed early on in the testing so we took that into account to determine the accuracy.

## 3.3 RQ2: Correction if an object passes through the line of sight.

This section investigates the feasibility of using HC-SR04 ultrasonic distance sensors to measure object thickness. The primary objective is to assess whether these sensors can accurately determine the thickness of objects that obstruct the line of sight between the sensors. This capability is useful for applications that require spatial tracking in dynamic environments. The thickness of the objects can be used to compensate for the distance measurements to find the real distance between the sensors.

### 3.3.1 Categorizing deviating measurements

The proposed method for measuring the thickness of objects using HC-SR04 sensors involves comparing actual measurements with expected values. In the direct method, both sensors should measure nearly equal distances between them. Significant discrepancies in these measurements indicate potential signal interference, as discussed in the previous chapter 3.2. This section categorizes these deviations to identify causes, providing insights into the disruptions in the measurement process.

We analyze variations observed during the direct method by categorizing deviations in sensor measurements effectively. These deviations include measurements that are shorter, slightly larger, significantly larger than anticipated, or cases where no measurement is detected. The following table 3 details the potential causes behind each category of deviation observed from the perspective of sensor 1.

Table 3: Analysis of Measurement Deviations

| **Measurement** | **Reason** | **Explanation** |
|---|---|---|
| Shorter | Object reflects sound | The object in front of sensor 1 reflects sound at least somewhat consistently. The part closest to sensor 1 is closer to sensor 1 than sensor 2; otherwise, the new measurements would be longer. This is because sound travels both ways in the reflective method. |
| Slightly larger | Curved signal | The signal from sensor 2 curves around the object, making the sound travel a longer route than the direct method. Ultrasound waves cannot curve sharply around objects and retain enough energy to be measured by the sensor. [**?**] |
| Slightly larger | Object in the middle | The object blocks the signal from sensor 2, reflects consistently, and the closest part that reflects the sound is near the middle of the two sensors, slightly towards sensor 2. |
| Significantly larger | No reflection | The object prevents sound from sensor 2 to reach sensor 1 directly. The object doesn't reflect sound, and the received signal is from another object. |
| Significantly larger | reflection | The object reflects sound from sensor 1, and the part that reflects the sound back to the sensor is closer to sensor 2. |
| No measurement | No reflection | The object between the sensors does not reflect sound and the sound from sensor 2 cannot curve around the object. |

### 3.3.2 Analysing measurements

By analyzing the measurements from both sensors, we can estimate what kind of object is between the two sensors. For example, say neither sensor was able to detect any sound. The object must be big enough for the sound to not curve around it. The object also could not reflect sound back to the sensor, there are multiple reasons this could happen. The first reason is that the object could reflect sound but the angle of the surface was not perpendicular to the sensor. The sound would have been reflected in a different direction than the sensor due to Snellius' law [Ope16b]. The second reason is that the object absorbed a large part of the sound and too little was reflected for the sensor to measure it [MKKB10]. The last reason is that the sound waves get scattered into too many directions and the sound waves that make it back to the sensor are too weak to be measured as an echo [MKKB10].

If the objective is to measure the thickness of the object between the sensors, both sensors must use the reflective method. This means the object must be able to reflect sound back to both sensors, and the sound waves from one sensor cannot be received by the other sensor before it has detected its own echo. There are two scenarios where the signal from one sensor might reach the other: the sound curves around the object or the object allows some sound to pass through it. The requirements for sound to pass through an object are complex, and out of scope for this thesis because during testing, we found that this occurred only with aluminum foil and paper: sound passes through thin objects easier [PN11].

### 3.3.3 Calculating the thickness

To calculate the thickness of an object let's take a barrier as an example that reflects sound back to the sensors, it doesn't let sound pass through it and is large enough so that sound does not curve around it. An example with a perfectly thin barrier placed in the center of two sensors is shown in 8. Had the barrier not been there, the sensors would have measured using the direct method, but now they are measuring using the reflective method. The key thing about this situation is that they still measure the same distance as if the barrier were not there. To mathematically prove, the following variable names shall be used:

- X = The distance between sensor 1 and the barrier
- Y = The distance between sensor 2 and the barrier
- Z = The distance between the two sensors
- A = Thickness of the barrier

$$\begin{aligned}\text{Total distance measured with barier} &= 2X + 2Y \\ &= 2(X + Y)\end{aligned}$$

$$\begin{aligned}\text{Total distance measured without barrier} &= 2Z \\ &= 2(X + Y + A) \\ &= 2(X + Y) + 2A\end{aligned}$$

Without the barrier, both sensors would be measuring Z, now sensor 1

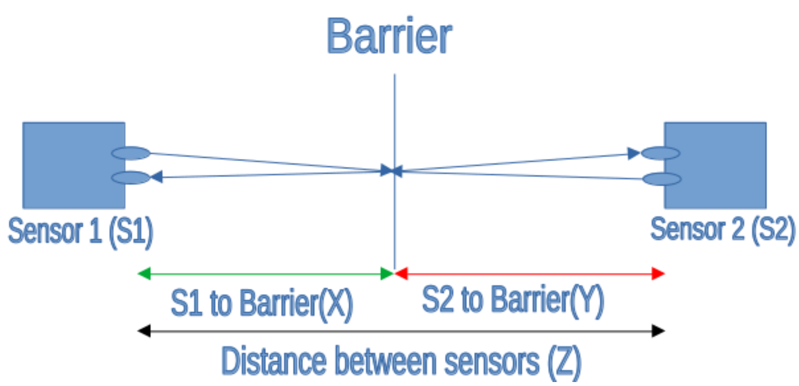


Figure 8: Perfectly thin barrier, breaking the line of sight

measures 2X and sensor 2 measures 2Y, as is seen in the mathamatical proof above. In this example X=Y=1/2Z, so they measure the same distance. In the second example as depicted in 9, the barrier does have a thickness. This means that the equivalence in distance measured is no longer true. The total distance between the sensors can now be written as Z=X+A+Y. The total measurement in the direct method can be written as 2Z = 2(X+Y) + 2A. The new total measurement is 2(X+Y), exactly 2*A or twice the thickness of the barrier fewer than the old total measurement. This is true for every barrier that reflects the sound back to the sensors, regardless of its position between the sensors. Furthermore, the position of the object between the sensors can also be inferred from the measurements. Since the sensors measure in the reflective mode, we know that the distance between the sensor and the object is half the distance measured because the sound has to travel both ways.

This research focuses on the use of ultrasound sensors in an indoor lo-

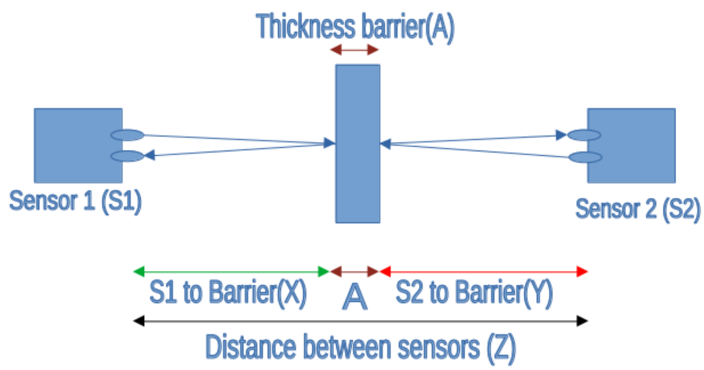


Figure 9: Barrier with thickness breaking line of sight

calization system where various objects could enter the area of interest. It is important to understand the reflectivity of the items that break the line of sight for determining whether their thickness can be accurately measured. Because it is unclear what kinds of objects might enter the area, items such as clothes and office supplies were tested to see if their thickness could be measured using the method that was just explained.

## 3.4 RQ3: Offset trigger moments/Accuracy retention without synchronized clocks

The proposed ultrasound system uses multiple Arduino's working together. Previously, we connected the sensors to the same Arduino, allowing us to trigger them simultaneously. However, once the sensors are connected to different microprocessors as depicted in Figure 10, ensuring a simultaneous trigger becomes challenging. Small timing errors can lead to significant measurement inaccuracies, necessitating a solution. In this section, we compare timing-synchronization solutions used by other systems and analyze what consequences an offset trigger moment has on the measurements.

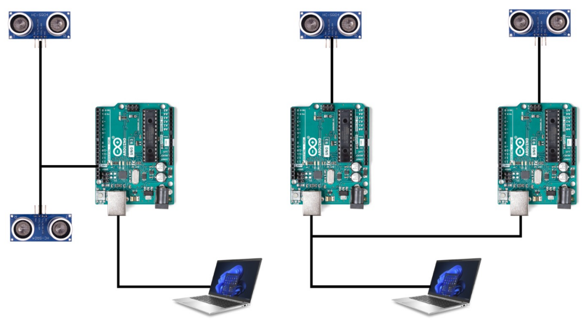

Figure 10: left, 2 sensors connected to 1 microprocessor
right, 2 sensors each connected to a microprocessor

#### 3.4.1 Synchronization in other systems

In various localization systems, accurate time synchronization is crucial for precise measurements. These systems rely on the principle of time of flight (ToF), which measures the time taken for a signal to travel from one sensor to another. To achieve this, the exact moments of signal transmission and reception must be noted and compared. However, when sensors are connected to different systems, their clocks may not be perfectly synchronized, leading to inaccuracies.

One solution to this problem is to synchronize the clocks of different systems. Some systems achieve this through WiFi, as noted in studies such as [QL17] and [LAY19]. GPS systems use highly accurate atomic clocks to maintain synchronization [BW99]. Another approach involves sending a radio frequency (RF) signal along with the ultrasound signal. The RF provides the required information of when the ultrasound signal was sent, while the ultrasound signal is used for distance measurement. This method is used by systems such as Zero Key to achieve high accuracy without synchronized clocks [DDM20].

Alternatively, some systems use a frequency hop system where the sensor can determine the moment the signal was send by the frequency of the received signal [SBBD12].

While these solutions can effectively address the synchronization issue, they often require additional equipment or more complex setups. The introduction of different types of sensors or ultrasound sensors that can determine frequency adds both complexity and cost, which we aim to avoid in our proposed system. Therefore, we seek a solution that maintains accuracy without the need for synchronized clocks or additional hardware.

### 3.4.2 Simultaneous trigger

To eliminate the timing issue, we first examine how the sensor operates in the reflective method, as shown in Figure 11.

In the reflective method, the sound is emitted at the trigger moment and

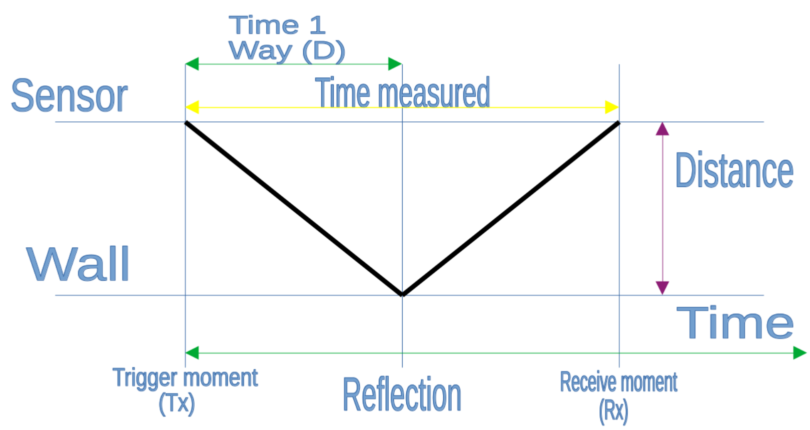


Figure 11: Reflective method schematic

travels at the speed of sound to the wall, where it gets reflected. Once the reflected sound reaches the receiver, the sensor stops measuring the time. Next, we compare this to the direct method using two sensors, as depicted in Figure 12.

In the direct method, the sound emitted by one sensor is received by the

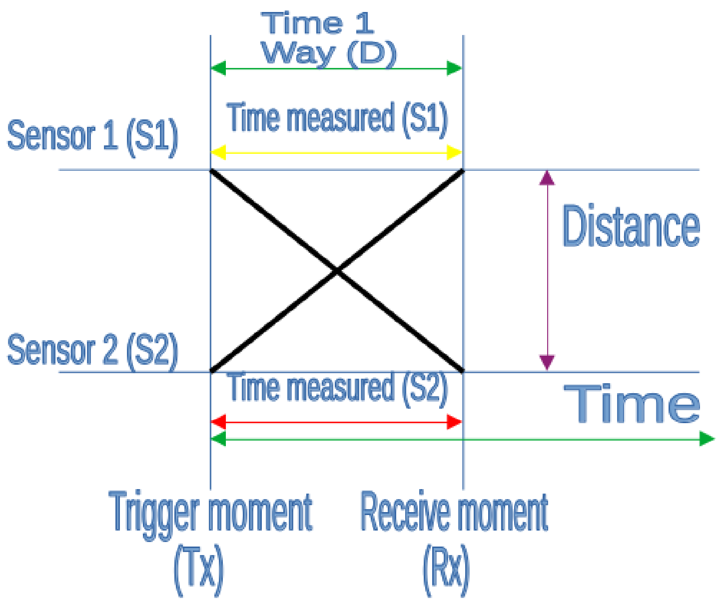


Figure 12: Direct method schematic

other sensor. Since the sound only travels the distance once, the time it takes is halved. This is how the sensors should work if they are triggered at the exact same time.

#### 3.4.3 Offset trigger

If the sensors are not triggered at the same moment, measurement inaccuracies can occur. Figure 13 illustrates this scenario, where sensor 1 is triggered at Tx1, and sensor 2 is triggered x seconds later at Tx2.

In this scenario, the time it takes for sound to travel the distance remains the same. The moment the signal reaches sensor 1 (Rx1) will be x seconds later, resulting in a measured time of (Rx1-Tx1), or in other terms, the time of one-way travel plus x. Since Tx2 was triggered x seconds later and Rx2 remains unchanged, the time measured by sensor 2 will be (Rx2-Tx2), or the one-way time minus x. By adding these two measurements, we eliminate x from the equation, obtaining twice the one-way travel time (equation 2).

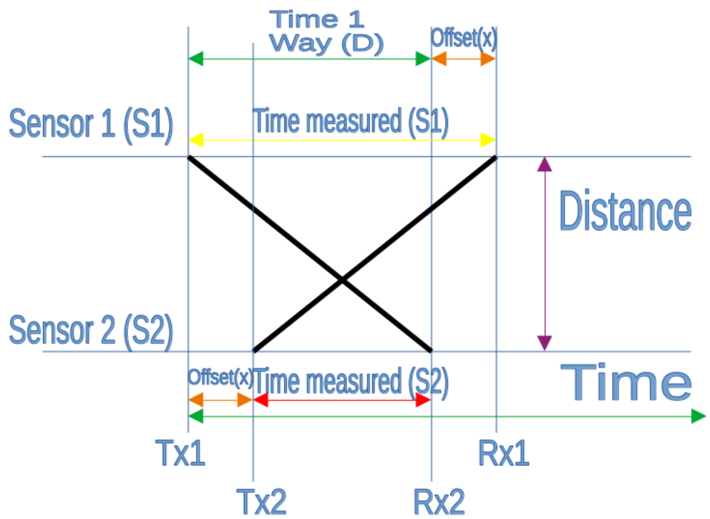


Figure 13: 2 sensors measuring in the direct method with offset trigger moments

This averaging method ensures measurement accuracy despite the lack of simultaneous triggering.

**Notation:** $c$ = Speed of sound

$$\begin{aligned}
\text{Total distance measured} &= \text{Measurement Sensor 1} + \text{Measurement Sensor 2} && (2)\\
&= (Rx1 - Tx1) \cdot c + (Rx2 - Tx2) \cdot c && (3)\\
&= (D + X) \cdot c + (D - X) \cdot c && (4)\\
&= 2D \cdot c && (5)\\
&= 2 \times \text{the distance between the sensors} && (6)
\end{aligned}$$

The trigger moment must be before the sound waves arrive at the sensor to ensure that the sensor is listening. The sensor begins listening for the echo after sending out 8 waves, which happens 10 microseconds after triggering the sensor [Unk1]. This trigger offset is therefore always small enough that it does not affect the time resolution, ensuring that the system's accuracy remains intact. To check if this method works a test similar to test 1 will be done so that this theory can be verified. The average of the measurements should be very similar if the distance between the sensors is the same.

## 3.5 RQ4: Can beacons be set up in any position without manual distance measure?

Automated calibration of beacons improves the accuracy and ease of deployment of an ultrasound system. Manually measuring the positions of each beacon can be time-consuming and mistakes can occur in the process. Such inaccuracies in calibration can lead to significant deviations in tag position calculations, making the system unreliable. Developing a method that allows beacons to autonomously determine their relative positions would eliminate this problem. Beyond calibration, the strategic placement of beacons is also vital for the system's overall effectiveness.

### 3.5.1 Beacon/Anchor and Tag/Mobile

A beacon, often referred to as an anchor in various research contexts, is a known and typically static sensor location that is used as a reference point in positioning systems. In the GPS localization system, for instance, satellites function as non-static beacons whose precise locations are continuously known [BW99].

In our research, we utilize beacons as fixed reference points that send and receive signals to and from the tag, or mobile unit, which is the object being tracked. The system relies on continuous communication between the tag and the beacons. Each beacon is equipped with two ultrasound sensors, each having a field of view of approximately 60 degrees. The decision to use two sensors per beacon was made to achieve a combined effective field of view of approximately 90 degrees. This overlap in the center provides redundancy which is useful for error detection. For now, consider the tag as an ultrasound sensor capable of sending and receiving signals in all directions. The detailed design and operation of the tag will be explained in section 3.6, an example of a beacon on a tripod is depicted in 14.

Figure 14: Beacon attached to a tripod

### 3.5.2 Beacon placement

The position of beacons is important for both the reliability and accuracy of the ultrasound positioning system. A minimum of three connections are required between the beacons and the tag to perform trilateration, allowing the system to determine the exact position of the tag.

Increasing the number of beacons can enhance both accuracy and coverage, as more beacons ensure the tag remains within range and line-of-sight of multiple beacons at all times. Furthermore, additional connections beyond the initial three can help detect faulty measurements and improve the overall accuracy. With more beacons, the system can perform additional trilateration calculations, leading to a more accurate average position by correcting individual sensor errors.

In our system, beacons must avoid reflective surfaces within their field of view to prevent measurement errors caused by reflected signals. For example, consider a scenario where beacon 1 and beacon 2 are trying to measure the distance between each other. The actual distance between them is 3 meters. If there is a reflective object, like a chair, positioned 1 meter from beacon 1, the sound waves emitted by beacon 1 could reflect off the chair and return to beacon 1 before the signal from beacon 2 is received. This reflection causes beacon 1 to measure an incorrect distance due to the reflected signal.

To mitigate this issue, beacons are placed higher up and tilted downward, a strategy also deployed by ZeroKey [DDM20]. This can help avoid problems from reflections of objects such as chairs or tables that are close to the floor. The increased height adds distance between the beacons and the object. Let us assume that the height increase causes the distance between beacon 1 and the chair to be more than 1.5 meters. Then the beacons would be able to measure using the direct method since the reflected signal now takes longer to reach beacon 1.

### 3.5.3 Scalability and formation

Previous research by Bas van Aalst has explored scalable setups for ultrasound systems [vA23]. One method involves arranging beacons in a trilateral constellation, which ensures that the tag is always within the range of at least three beacons. For our research, we focus on a smaller area using just three beacons, the absolute minimum.

An equilateral triangle setup is optimal because it maximizes the area covered while minimizing the number of beacons. Each corner of the triangle has an angle of 60 degrees, which means one sensor on each beacon is sufficient to cover the entire area within the triangle. The design of our beacons, where the angle between the sensors is 60 degrees, ensures that the sensors on the beacons face each other directly.

This setup not only provides accurate tracking within the initial area but also allows for easy scalability. By following Bas van Aalst's design principles, our beacon system can be expanded to cover a larger area without significant changes to the design; more sensors should be attached so that it has a 360-degree field of view [vA23]. The direct method allows for longer-range measurements, reducing the number of beacons required per surface area.

### 3.5.4 Calibration

As mentioned earlier, accurate calibration of beacons is crucial for the effectiveness of any ultrasound positioning system. Manual calibration is time-consuming and prone to errors, leading to significant deviations in tag position calculations. To address this, it is essential to use a method where beacons autonomously determine their relative positions. Research has been done on self-calibration methods, such as Distribute & Erase and Explorer, which aim to automatically determine anchor positions within a room [RBK11]. For this research, only the relative position of the beacons is required.

In our system, the calibration process begins with each beacon measuring the distances to all other beacons. Once the distances are obtained, we establish a fixed coordinate system for relative positioning. Beacon 1 is set at the origin (0,0,0), and Beacon 2 is positioned along the x-axis at (X,0,0), where X is the distance measured between Beacon 1 and Beacon 2. To find the position of Beacon 3, we assume all beacons are at the same height, simplifying the calculation to a two-dimensional plane. Using the measured distances and basic trigonometric principles, we can determine the coordinates of Beacon 3 as (B,A,0), where A and B are derived from the known distances between the beacons.

If the heights of the beacons are not equal, additional calculations are necessary after determining the coordinates using the previously described method. To account for the difference in height, the Pythagorean theorem can be applied to adjust the X-coordinate of Beacon 2.

$$(\text{height Beacon 1} - \text{height Beacon 2})^2 + X_{\text{actual}}^2 = X_{\text{calculated}}^2$$

A similar approach can be applied to adjust the coordinates of Beacon 3, taking into account its height difference relative to the other beacons.

To validate our calibration method, a test will be conducted where the beacons are deployed as they would be in a real tracking scenario. The program will determine the locations of the beacons, which will then be compared to their actual positions to assess the accuracy of the automatic calibration process.

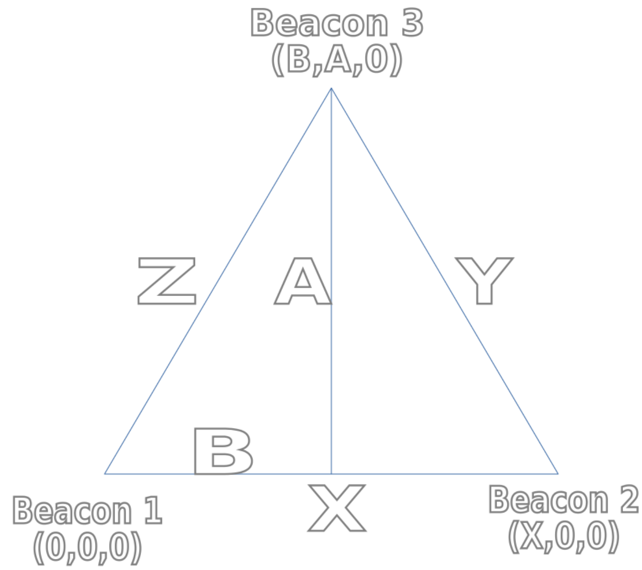


Figure 15: Euclidean beacon Locations at the same height

## 3.6 RQ 5 and 6: System design to calculate the location and orientation of the tag

In this chapter, we delve into the workings of the tracking system and its intended capabilities. The primary objective of this system is to accurately track the location of the tag. In addition, it aims to assess the planar orientation of the tag, a feature that improves the usability of the system. These objectives for advancing the system developed by Bas van Aalst could enable it to replace the UWB system by Pozyx in various scenarios. The ultrasound system is anticipated to offer benefits such as cost-effectiveness, ease of deployment, and enhanced accuracy over the UWB system. Testing will be conducted to evaluate the system's accuracy and its ability to determine orientation.

### 3.6.1 System overview

The ultrasound tracking system is composed of three beacons and a tag connected to a computer via USB cables. Research suggests that replacing USB cables with Wi-Fi connectors could potentially reduce interference and extend the operational range, enhancing the system's robustness and versatility [QL17] [DDM20]. While the addition of Wi-Fi connectivity might slightly increase costs, the modules are relatively inexpensive, making this a viable option for improving the system without adding significant complexity. The beacons are fixed reference points that communicate continuously with the mobile tag to determine its position and orientation. Each beacon in our system consists of two ultrasound sensors attached to an Arduino. Referring to the setup described in RQ4 3.5, the beacons are arranged in a perfect triangular formation to ensure line of sight with the tag at each point within the triangle and to minimize signal interference.

The tag is the mobile unit whose position and orientation are tracked, as depicted in figure 16. The tag is equipped with six ultrasound sensors, arranged to provide a full 360-degree field of view. Each sensor is positioned 9 centimeters from the center of the tag and faces outward. Although each sensor is most sensitive within a 30-degree range, the direct method employed in this system provides a total field of view of 60 degrees per sensor pair, as discussed in Section 3.2.2. This arrangement ensures complete coverage around the tag, allowing it to maintain line of sight with all the beacons at all times. The sensors are also tilted slightly upward to optimize signal reception and transmission, since the beacons are positioned higher than the tag in all tests.

Within the tracked area, the angle between the tag and any two beacons will always exceed the 60-degree range of the sensors. This insight, combined with the fact that the sensors have a 60-degree operating range, means that no two beacons will target the same sensor on the tag. This ensures that each beacon establishes a unique connection with a specific sensor on the tag. These unique connections allow our system to replicate the UWB system's functionality, determining the planar orientation of the tag.

The software for this system can be grouped into three sections: the python program that sends and receives to the Arduino's, the c files that get uploaded to the Arduino's that trigger the sensors and the Python program that uses all the measurements to calculate the location of the tag. [2]

[2] The source code and related files can be found at: https://github.com/Wearable-Data-Observatory-Leiden/PositioningWithUltrasound/tree/main/

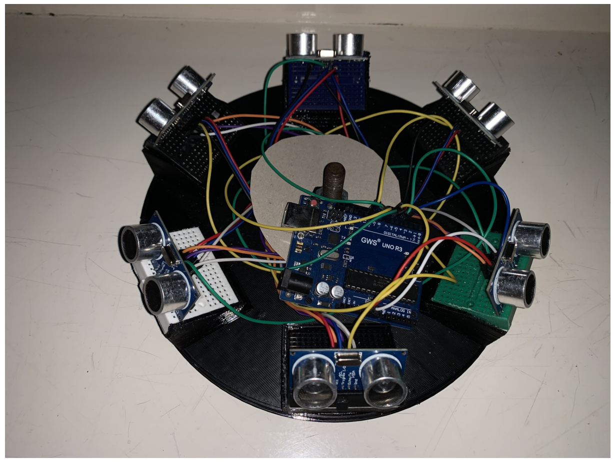

Figure 16: Tag with connected sensors

### 3.6.2 Setup Phase

The setup phase is split into two parts. The first part involves the calibration of the beacon locations, as discussed in the previous chapter 3.5. The second part focuses on tag calibration, specifically the creation of a lookup table containing the differences between measurement for each sensor pair. This lookup table is essential for later determining which sensor on the tag is facing which beacon.

During testing of the direct method, we observed that sensor pairings can influence the measurements made by the sensors. This variation in the measurements was significant and consistent enough to require a correction. To address this, the tag was placed in the center and rotated so that each sensor could face all other sensors and make measurements. The differences in the distances measured by each sensor pair are then into a lookup table. A condensed version is shown in Figure 17.

### 3.6.3 Cycle of measurements

After the setup phase, the process of tracking the tag's location can begin. A sketch of the beacons and the tag, illustrating the arrangement and positions

fIles_used_for_each_test/Test5.

| | Beacon 1 | Beacon 2 | Beacon 3 |
|---|---|---|---|
| Tag sensor 1 | 26.3 | 21.7 | 8.2 |
| Tag sensor 2 | 29.3 | 22.2 | 11.8 |
| Tag sensor 3 | 29.2 | 19.3 | 12.1 |
| Tag sensor 4 | 30.8 | 20.7 | 14.2 |
| Tag sensor 5 | 27.5 | 19.5 | 11.3 |
| Tag sensor 6 | 28.6 | 18 | 10.2 |

Figure 17: Lookup table filled in

of the sensors, is shown in Figure 18. The control program sends a signal to the Arduinos, and each makes a measurement. The tag has six sensors, with only one sensor measuring at a time, so six measurements are needed to complete one cycle. Each measurement takes slightly longer than 0.1 seconds, and a cycle is completed in approximately 0.62 seconds. The beacons have only two sensors, so they each make three measurements per cycle. An example of all measurements in a cycle is depicted in 19.

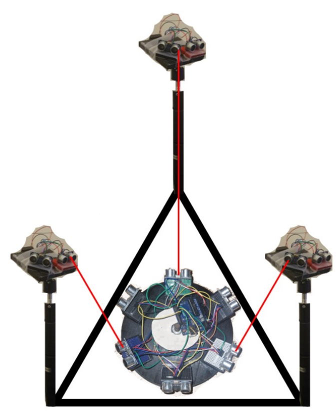

Figure 18: Setup of 3 beacons making a connection to the tag

### 3.6.4 Finding the connections

After completing the measurement cycle, the next step is to determine the distances between each beacon and the tag. To do this, we must first identify

| Beacon1 s1 | Beacon1 s2 | Beacon2 s1 | Beacon2 s2 | Beacon3 s1 | Beacon3 s2 | tag s1 | tag s2 | tag s3 | tag s4 | tag s5 | tag s6 |
|---|---|---|---|---|---|---|---|---|---|---|---|
| 177.6397 | | | | | | | | | | | |
| | | 185.8717 | | | | | | | | | |
| | | | | 149.5137 | | | | | | | |
| | | | | | | 183.4021 | | | | | |
| | 213.5861 | | | | | | | | | | |
| | | | 172.8377 | | | | | | | | |
| | | | | | 148.0045 | | | | | | |
| | | | | | | | 166.2521 | | | | |
| 181.4813 | | | | | | | | | | | |
| | | 187.6553 | | | | | | | | | |
| | | | | 147.5929 | | | | | | | |
| | | | | | | | | 208.6469 | | | |
| | 210.0189 | | | | | | | | | | |
| | | | 171.8773 | | | | | | | | |
| | | | | | 146.2209 | | | | | | |
| | | | | | | | | | 140.4585 | | |
| 179.6977 | | | | | | | | | | | |
| | | 187.2437 | | | | | | | | | |
| | | | | 148.1417 | | | | | | | |
| | | | | | | | | | | 138.4005 | |
| | 219.2113 | | | | | | | | | | |
| | | | 162.9593 | | | | | | | | |
| | | | | | 146.2209 | | | | | | |
| | | | | | | | | | | | 148.9649 |

Figure 19: Full cycle of measurements

the correct sensor-beacon pairings.

For this purpose, we use the lookup table created during the setup phase. This table contains the expected differences in measurements between each sensor pair. For example, if we are assessing whether sensor 1 is facing beacon 1, we calculate the difference in distance measured between beacon 1 and sensor 1 (let's say this is 30 cm). We then compare this difference with the expected difference from the lookup table for the pair (sensor 1, beacon 1), which is 26.3 cm. In this case, the difference between the actual and expected values, or the error, is 3.7 cm.

Each potential pairing scenario is evaluated based on these errors. We calculate an error score for each scenario by comparing all the measured differences to the expected differences in the lookup table. Scenarios with smaller errors are more likely. After evaluating all possible scenarios, the most likely sensor-beacon connections are identified, and these connections are used to calculate the tag's location.

### 3.6.5 Calculation of the location

Once the connections are determined, the average distance of each sensor pair is calculated and used in the trilateration formula. Initially, the calculated location was displayed in real-time; however, controlling the Arduino's, calculating the location, and displaying the plot simultaneously proved too computationally intensive for the used laptop. Now, the calculations are made after all the measurements have been made.

The useful measurements in each cycle are utilized once, resulting in a refresh rate of approximately 0.62 seconds. This refresh rate could be improved by using the measurements more than once or estimating the distance between a beacon and a tag at a specific moment using previous and subsequent measurements. Testing involves a train moving in a circle at a steady speed, with the tag attached to the top of the train. This setup ensures that the tag's location is known at all times, so that the actual and measured distances can be compared.

#### 3.6.6 Orientation

The orientation is calculated using the location of the tag and the connections between the beacons and the tag. For example, in 20, sensor 1 of the tag faces beacon 1, sensor 3 faces beacon 2, and sensor 5 faces beacon 3. Given these connections and the location of the tag, the tag's representation is correctly shown. The orientation accuracy is within $\pm 30$ degrees; if the tag rotates more than 30 degrees in either direction, sensor 1 will no longer face beacon 1. This rotation property is true for at least one sensor of the tag at any location within the perfect triangle. Therefore, no matter where the tag is, the accuracy of the estimated orientation should be within $\pm 30$ degrees. After the location of the tag on the train is calculated the orientation is calculated to test whether this method works.

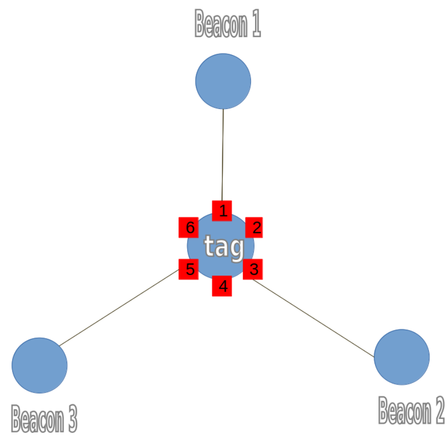


Figure 20: Tag with 3 connections to the beacon

# 4 Experiments

## 4.1 RQ1 test 1: accuracy measurement direct method

The goal of this test is to determine the accuracy of the HC-SR04 sensors when configured with the direct method. Following the principles established by Fuad Aliew's research [Ali22], we implemented a setup where two sensors are connected to the same Arduino and positioned to face each other, as shown in Figure 21. The Arduino is connected to a laptop for data collection and to upload the test file, test1New.ino, which is found in the project repository. This file triggers sensor 1 and sensor 2 in an alternating loop at 50 ms intervals. The 50 ms interval is selected to maximize the number of measurements within the given time frame while ensuring reliable operation of the sensors. [3]

Both sensors are connected to the same trigger pin on the Arduino. When the program triggers a sensor, current runs through the trigger pin, causing both sensors to send a signal. However, only the sensor that is intended to make a measurement keeps its trigger pin high until it receives an echo 3.1.

[3] The source code and related files can be found at: https://github.com/Wearable-Data-Observatory-Leiden/PositioningWithUltrasound/tree/main/files_used_for_each_test/Test1.

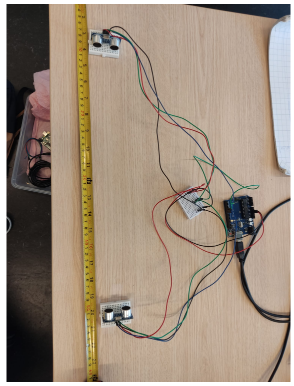

Figure 21: 2 sensors facing each other

The sensors were positioned at distances of 20, 50, 100, and 200 centimeters from each other. At each distance, the base sensor was tested against five different sensors to eliminate a possible sensor pairing bias. This is done because early testing showed that different sensor pairs at the same positions measured a different distance. Measurements were taken from the first to the sixty-first second, as the initial measurement - the first distance - is often faulty, likely due to the starting up of the program. The tests were conducted at a temperature of 20 degrees Celsius.

## 4.2 RQ2 test 2: thickness measurements of different objects between two sensors

To determine whether HC-SR04 ultrasonic sensors can measure the thickness of objects accurately, we conducted a series of tests using two sensors set up in the direct method at a distance of 40 centimeters apart. The Arduino file used for this setup, named 2sensors.ino, is available in the project repository. This file alternately triggers sensor 1 and sensor 2 in a loop with 50 ms intervals. The real-time distance measurements were streamed from the Arduino to a laptop, allowing us to monitor them. Initially, baseline measurements were taken to establish a reference point. Then, various objects were placed between the sensors, positioned 13 cm from sensor 1. The new measurements from both sensors fell into one of four predefined categories 3, which were then recorded in a table. The objects tested included aluminum foil, a sock, a tennis ball, an apple, a tape holder, a fuzzy hat, and a notebook. During testing, we observed some interesting properties with the notebook and the tennis ball, prompting us to test them twice. The notebook exhibited different behavior when tightly shut compared to when there was some air between the pages. The distance between the tennis ball and the sensors influenced the measurements.

## 4.3 RQ3 test 3: accuracy measurement direct method 2, using multiple Arduino's

In this test, the sensors are facing each other at a predefined distance. There are four distances tested: 20, 50 , 100, and 200 cm. One sensor was selected - the base sensor - and the distance between five different other sensors were measured. Unlike the previous test (RQ1 test1), the sensors are connected to two separate Arduino boards.

Both Arduino boards are connected to the same laptop, and the file test2New.ino is uploaded to both. This file ensures that each Arduino waits for an input signal, measures the distance once upon receiving the signal, and sends the data back to the laptop. The laptop sequentially sends the signal to both Arduino boards with a variable delay of approximately 3 milliseconds, waits for 100 milliseconds, and then collects the data from both Arduinos. This process loops continuously for one minute. [4]

Measurements are taken at each distance and the base sensor is tested against five different sensors. Data collection starts after the first second and continues until the sixty-first second, excluding the initial measurement since this is usually incorrect. The tests are carried out at a temperature of 20 degrees Celsius.

[4]The source code and related files can be found at: https://github.com/Wearable-Data-Observatory-Leiden/PositioningWithUltrasound/tree/main/flles_used_for_each_test/Test3.

## 4.4 RQ4 test 4: beacon calibration

The objective of this test is to validate the automatic calibration of the beacons. Each beacon consists of two sensors connected to an Arduino, positioned at a 60-degree angle relative to each other. The Arduino's are connected to a laptop, and the 2sensors.ino file is uploaded to all Arduino's. A Python script is used to control the Arduino's, sending signals that indicate which sensor (1 or 2) should be triggered. When a sensor is triggered, both sensors connected to the Arduino emit an ultrasound signal, but only the triggered sensor waits for the echo to return. It is not needed in this test for the sensor that is not receiving the signal to send out a signal but shouldn't interfere and will be useful in later tests.

Initially, sensor 1 of beacon 1 and sensor 2 of beacon 2, which are facing each other, are repeatedly triggered to gather distance measurements. After sufficient measurements are collected, the last X measurements are used to determine the distance between these sensors. This process is repeated for all pairs of sensors to determine the distances between the beacons. Once all distances are measured, the beacon locations are calculated in Euclidean coordinates and compared to their actual positions. Different setups are tested, but for conciseness, only the results where the beacons are placed 3 meters apart and at the same height are analyzed.

## 4.5 RQ5 test 5: tracking moving target

This test aims to assess the accuracy of tracking the location and orientation of a moving tag using a setup of three beacons. The beacons are arranged in an equilateral triangle, each side measuring 3 meters. The tag is mounted on a train that moves along a circular track with a diameter of 86 cm, positioned precisely at the center of the triangular arrangement of the beacons. The train with the attached tag, and the track in detail, is depicted in Figure 22. Figure 23 shows a broader view of the test setup, including two of the three surrounding beacons.

Before the train starts moving clockwise around the track, the beacons perform an initial calibration by measuring the distances between each other to confirm their positions. Following this, the system enters a second calibration phase, where each combination of beacon sensor and tag sensor is

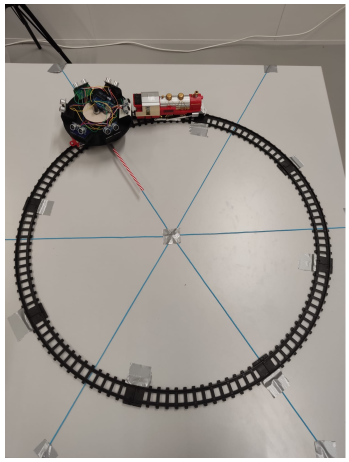

Figure 22: Train with tag attached to it

Figure 23: Train in between 3 beacons, only 2 could fit the picture

calibrated. During this phase, the differences in sensor readings are recorded and will later be used to generate a lookup table after the test is completed. Once the calibration steps are completed, the test proceeds with the measurement cycles. During this phase, all four Arduino boards continuously trigger their sensors in a loop. The beacons alternate between triggering their sensors, while the tag cycles through its six sensors in sequence, as detailed in Section 3.6. The goal is to achieve the highest possible time resolution, which, in this setup, is approximately 0.62 seconds. An example of a filled-in measurement cycle is shown in Figure 19. The train then starts its movement along the circular track at a nearly constant speed, where the variance in lap time is within half a second.

### 4.5.1 Data Processing

After the test is completed, the collected data is processed. The first step is to use the measurements from the beacon calibration phase to calculate the exact positions of the beacons. Following this, the differences in sensor measurements recorded during the sensor pairing calibration are used to generate a lookup table, as described in 17. This lookup table contains the differences in measurements for each sensor pairing. The dataset is then pruned, removing any data that was collected during the setup phase, leaving only the measurements taken while the train was in motion. For each cycle of measurements, the most probable sensor connections are identified using the lookup table. If no probable combination is found, meaning the differences between the sensor pairs deviate too far from the values in the lookup table, the distances for that cycle are not calculated. Only the data from the most likely connections are retained, and these values are averaged to calculate the distances between the tag and each beacon. Since the tag's sensors are positioned 6 cm away from its center, a correction of 6 cm is added to each calculated distance. The resulting data is separated into two sets: one containing the distance measurements along with timestamps and the other containing the sensor connections and timestamps.

### 4.5.2 Location Calculation

Using the distances file, the program calculates the position of the tag for each cycle based on the distances between the tag and the beacons. The triangulation method used for these calculations is described in 3.6. After calculating the positions for each cycle, the program adjusts the start time by testing different moments to minimize the positional errors across the entire dataset. Once the optimal start time is determined, the errors associated with the calculated positions are analyzed to assess the system's accuracy.

### 4.5.3 Orientation Calculation

The connections file is analyzed to determine the accuracy of the system in tracking the tag's orientation. Expected sensor connections are calculated based on the tag's position and orientation. The program synchronizes the timestamps and compares the actual sensor connections with the expected ones, assessing how often the correct connections were made and thereby evaluating the accuracy of the orientation tracking.

# 5 Results

## 5.1 Results of RQ1 test 1: accuracy measurements direct method

The results of test one for each distance and sensor combination are visualized in Figure 24 where the actual distances are the horizontal lines and the average of the measurements over the period of time are represented in bars. The summary of the difference between the measured and actual distances is represented in Table 4.

At the shortest distance of 20 cm, the highest percentage of difference

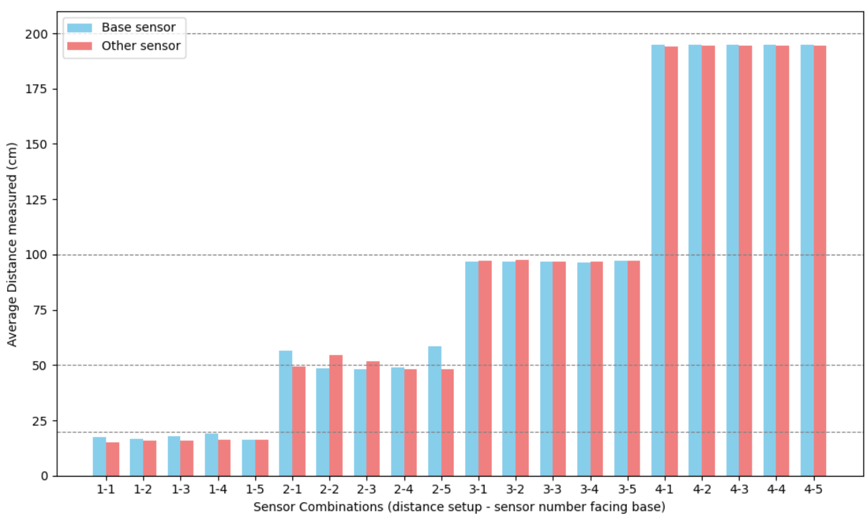


Figure 24: Average distance measured over a minute by each sensor

Table 4: Average of all measurements at each distance

| Distance number | Actual (cm) | Measured (cm) | Avg difference to actual (cm) | Percentage off (%) | Variance ($cm^2$) |
|---|---|---|---|---|---|
| 1- | 20 | 16.658 | 3.342 | 20.06 | 487.57 |
| 2- | 50 | 51.255 | 3.020 | 6.40 | 4979.58 |
| 3- | 100 | 96.883 | 3.117 | 3.22 | 158.15 |
| 4- | 200 | 194.567 | 5.433 | 2.79 | 120.65 |

between the actual and the measured distance was found while at 50 cm the distance measurements on average exceeded the actual distance and had by far the highest variance. After collecting the data and seeing the high variance at 50 cm the test was repeated at that distance to verify whether something had gone wrong, the results were similar. For the actual distances of 100 cm and 200 cm, the results were similar and showed the most consistent measurements albeit about 3 percent below the actual distance. Due to the sensors underestimating the distance of 3 percent the test at the largest distance had the highest absolute difference.

The measurements over time of combinations 1-1 and 4-1 are represented in figure 25 and figure 26 in the same manner that Fuad Aliew has visualized his results. This is done so that the results of the direct method can be compared to the reflective method. Here we can see that the measurements over time were quite consistent and the measurements seem to correspond with those found in the research of Fuad Aliew. [Ali22].

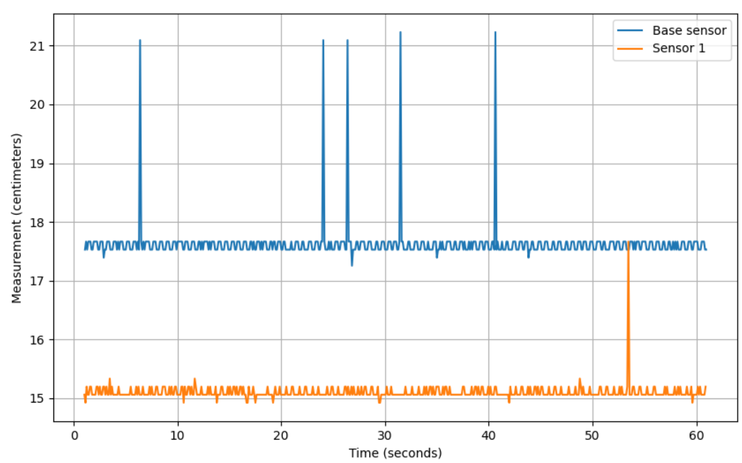


Figure 25: Distance between base sensor and sensor 1 at 20 cm

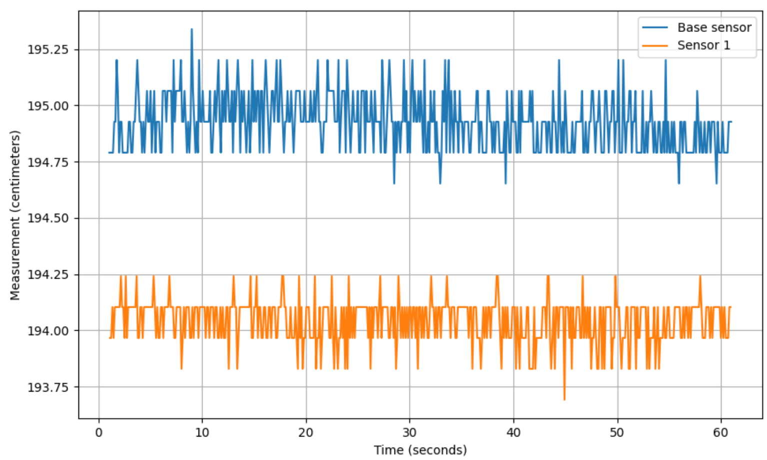


Figure 26: Distance between base sensor and sensor 1 at 200 cm

## 5.2 Results of RQ2 test 2: the thickness of objects in line of sight

The table of the measured distances by both sensors is depicted in figure 27. The properties of the objects varied significantly, with only one object reflecting sound to both sensors. Sound tended to curve around most of the small objects, leading to a slight increase in the distance measured by sensor 1. The tennis ball showed different results based on its position: when placed in the center (Tennis ball (far)), it showed no reflection for either sensor. However, when placed at a distance of 10 centimeters from sensor 2 (Tennis ball (close)), it reflected sound to the sensor.

The aluminum foil and tightly closed notebook allowed a fraction of the sound to pass through and another fraction to reflect back to sensor 2 because they are thin. When the notebook had more air between the pages (Notebook (loose)), the additional air acted as an insulating layer, disrupting sound transmission resulting in the sound waves no longer passing through.

| | Disance measured sensor 1 (object far) | | | | Disance measured sensor 2 (object close) | | | |
|---|---|---|---|---|---|---|---|---|
| Item between sensors: | Line of Sight | Line of sight+ | NaN | Object | Line of Sight | Line of sight+ | NaN | Object |
| Aluminum foil | x | | | | | | | x |
| Sock | | x | | | | x | | |
| Apple | | x | | | | | | x |
| Tape holder | | x | | | | | | x |
| Tennis ball(far) | | x | | | | x | | |
| Tennis ball(close) | | x | | | | | | x |
| Hat | | | x | | | | x | |
| Notebook(tight) | x | | | | | | | x |
| Notebook(loose) | | | | x | | | | x |

Figure 27: Reflectivity of various objects

## 5.3 Results of RQ3 test 3: accuracy measurement triggers

The results of test 3 at each distance and sensor combination are visualized in Figure 28. The actual distances are represented by the horizontal lines, and the average of the measurements over the test period are shown as bars. Table 5 provides a summary of the difference between the actual and measured distances.

At the shortest distance of 20 cm, the highest percentage of difference between the actual and measured distances was found. At 50 cm, the measurements on average exceeded the actual distance, similar to test 1. At 100 cm, the lowest absolute difference to the actual distance was recorded, while at 200 cm, the lowest percentage difference was observed. The highest variance was measured at the largest distance due to an outlier in test 4-4, where both sensors measured an unusually high distance once.

Table 5: Measurement Results test 3

| Actual (cm) | Measured (cm) | Avg difference to actual (cm) | Percentage off(%) | Variance ($cm^2$) |
|---|---|---|---|---|
| 20 | 17.460 | 5.592 | 27.96 | 5231.97 |
| 50 | 50.907 | 5.720 | 11.44 | 5956.66 |
| 100 | 96.293 | 4.436 | 4.44 | 1279.47 |
| 200 | 194.979 | 7.329 | 3.66 | 14172.42/2467.96* |

The measurements over time for combinations 1-1 and 4-1 are represented in Figures 29 and 30. In these figures, it is evident that the measurements over time differ significantly from test 1. In test 1, each sensor provided more consistent measurements. However, in Test 3, the measurements showed greater variability from one to the next. In test 4-1, there are notable peaks and corresponding valleys, such as at the 10-second mark where the blue line peaks, and immediately afterward, the orange line drops. This pattern indicates that when sensor 1 measures a higher value, sensor 2 tends to measure a lower value, reflecting the expected behavior due to the slight discrepancies in trigger moments in the direct method.

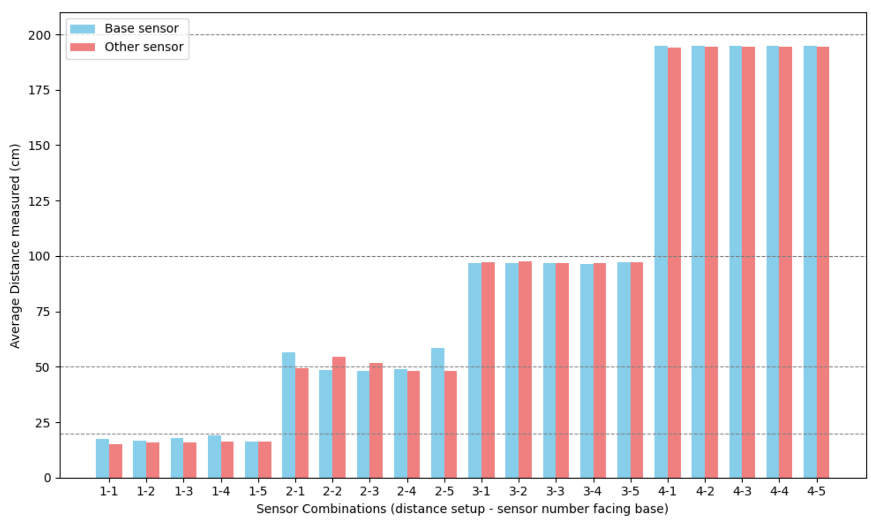


Figure 28: Results all sensor pairings

## 5.4 Results of RQ4 test 4: beacon calibration

The results of Test 4, where the distances between the beacons were measured, are summarized in Table 6. Each test was conducted with the beacons placed at 3 meters apart, and the measurements were taken using three different trials to ensure accuracy. The measurements were generally consistent across the tests, with the maximum difference in the average distance measured

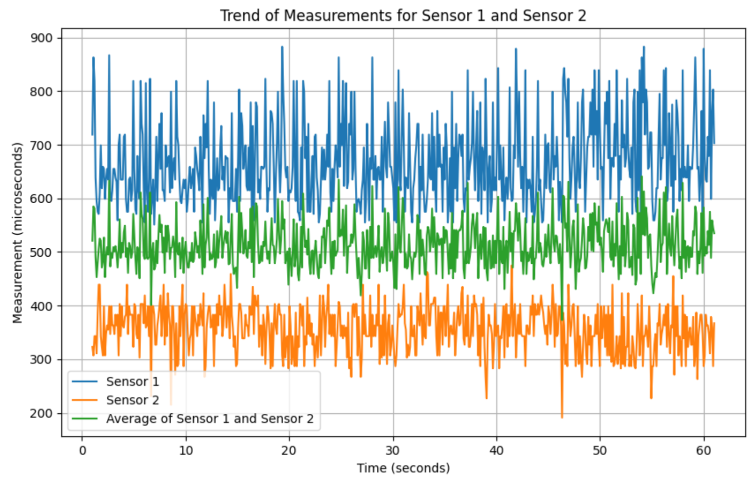


Figure 29: Results sensor pairing 1-1

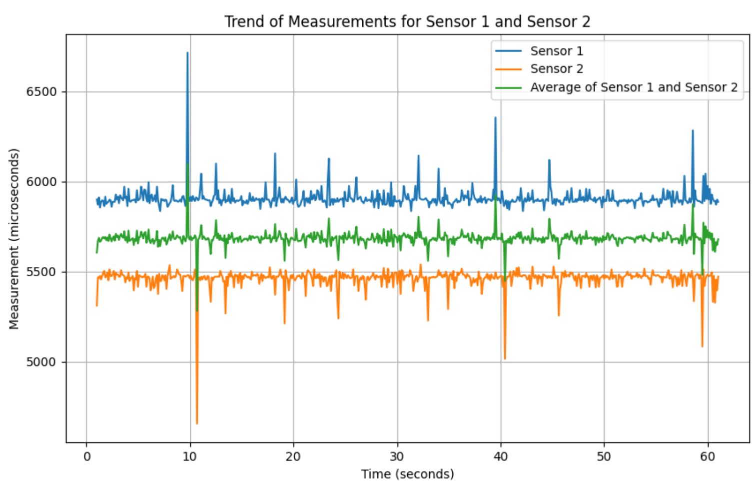


Figure 30: Results sensor pairing 4-1

Table 6: Measured Distances Between Beacons

| Sensor Pair | Test 1 (cm) | Test 2 (cm) | Test 3 (cm) |
|---|---|---|---|
| B1-B2 | 295.18 | 295.71 | 294.63 |
| B1-B3 | 294.12 | 294.07 | 294.14 |
| B2-B3 | 298.44 | 298.55 | 298.61 |

Table 7: Coordinates of Beacon 3

| | X-Coordinate | Y-Coordinate | Distance to actual (cm) |
|---|---|---|---|
| Test 1 | 143.25 | 256.88 | 7.36 |
| Test 2 | 143.36 | 256.76 | 7.31 |
| Test 3 | 142.82 | 257.14 | 7.16 |
| Actual | 150.00 | 259.81 | 0 |

being 1.08 cm, which is small but significant. All the averages were below the expected measurements. This is not surprising since all measurements using the direct method were lower for distances above 1 meter, as seen in Test 1 and Test 3. The lower measurements resulted in significantly miscalculating the X and Y coordinates, but they did result in consistent coordinates. Individual measurements varied up to 14 centimeters, as seen in Figure 31; this was anticipated based on the results of Test 3, where the trigger moments are offset in both tests.

## 5.5 Results of RQ5 test 5: accuracy over time

In this section, we analyze the accuracy of the tag's location tracking across three runs. The analysis focuses on two aspects: the precision of the measured positions and the success rate of measurement cycles that resulted in a calculated location. It's important to note that this section exclusively addresses location tracking, while orientation tracking is analyzed separately.

The calculated positions of the tag during the first lap of Run 1 are visualized in Figure 32. In this figure, the green dots represent the measured positions, while the red dots indicate the actual positions the tag was supposed to be in. The lines connecting these points illustrate the error for each

| | Last 5 measurements made per sensor | | | | | |
|---|---|---|---|---|---|---|
| | B1S1 | B1S2 | B2S1 | B2S2 | B3S1 | B3S1 |
| Test 1 | 304.0009 | 316.6233 | 305.2357 | 286.3021 | 271.2101 | 291.7901 |
| | 302.3545 | 301.9429 | 312.6445 | 290.2809 | 286.0277 | 284.1069 |
| | 304.6869 | 302.3545 | 305.9217 | 285.4789 | 285.7533 | 291.1041 |
| | 302.0801 | 304.8241 | 304.5497 | 287.2625 | 284.2441 | 292.3389 |
| | 309.7633 | 310.5865 | 303.5893 | 279.5793 | 277.6585 | 293.1621 |
| | | | | | | |
| Test 2 | 304.1381 | 298.7873 | 306.1961 | 289.4577 | 289.3205 | 290.9669 |
| | 310.4493 | 299.8849 | 306.8821 | 278.8933 | 288.2229 | 290.1437 |
| | 304.8241 | 304.5497 | 304.4125 | 288.7717 | 283.6953 | 291.9273 |
| | 301.6685 | 298.6501 | 307.8425 | 286.0277 | 289.3205 | 289.4577 |
| | 303.4521 | 299.0617 | 306.8821 | 289.4577 | 289.1833 | 290.8297 |
| | | | | | | |
| Test 3 | 304.9613 | 300.0221 | 305.5101 | 285.2045 | 288.0857 | 292.3389 |
| | 304.0009 | 299.1989 | 306.3333 | 286.1649 | 289.0461 | 290.6925 |
| | 302.4917 | 299.4733 | 306.0589 | 289.4577 | 289.4577 | 291.2413 |
| | 299.7477 | 299.8849 | 308.1169 | 286.8509 | 288.2229 | 288.9089 |
| | 300.9825 | 298.9245 | 305.7845 | 286.4393 | 289.0461 | 291.1041 |

Figure 31: All measured distances

measurement. Run 1 is depicted in Figure 33, where all measured points, the actual trajectory of the train and the positions of the beacons are shown. All runs have the same characteristic of the points furthest from beacon 1 not being far enough from beacon 1. To quantify the accuracy of the location tracking, the average error of the measurements was calculated for each of the three runs. The average error represents the Euclidean distance between the calculated and actual positions, averaged over all successful measurements within a run. The results are summarized in the following table 8: The table

Table 8: Average positioning errors across all runs

| Run | Number of Measurements | Average Error (cm) |
|---|---|---|
| 1 | 88 | 7.17 |
| 2 | 79 | 8.48 |
| 3 | 51 | 7.21 |
| Overall | 218 | 7.65 |

8 shows the average error for each run, highlighting the consistency of the tracking system's performance across different trials. The overall average

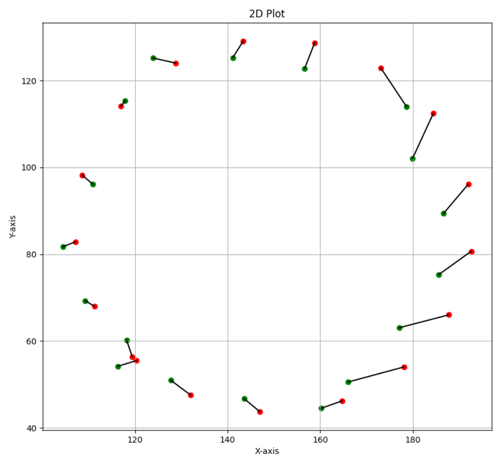


Figure 32: Locations calculated (green dots) compared to the actual locations (red dots)

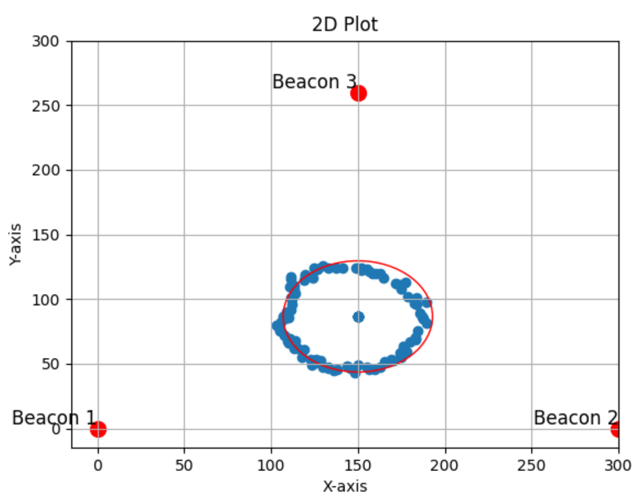


Figure 33: All calculated loctions of the first run

error, calculated by taking the mean of the average errors from all three runs, is 7.21 cm.

In addition to assessing positional accuracy, we also evaluated how many measurement cycles resulted in successful sensor pairings. Remarkably, every single measurement cycle across all three runs resulted in a successful pairing, meaning the system consistently identified the correct sensor connections for every cycle.

## 5.6 Results of RQ6 test 6: orientation of the tag

In this section, we analyze the accuracy of the orientation tracking of the tag during the first run. Due to a human error, where a bolt was not properly tightened, the tag rotated relative to the train in subsequent runs, making the data from those runs unreliable. Therefore, only the first run is analyzed.

Figure 34 illustrates the sensor pairing data for the first run, highlighting the alignment between the actual tag sensor facing each beacon and the sensor pairing detected by the system. The figure analyzes the results from the first 24 measurement cycles. In the figure green cells represent correct pairings, where the beacon correctly identified the tag sensor directly facing it. Yellow cells indicate a pairing where the beacon identified a tag sensor adjacent to the correct one (e.g., if Beacon 1 was supposed to pair with Tag Sensor 2 but instead paired with Tag Sensor 3). Red cells show pairings where the beacon identified a tag sensor two positions away from the correct sensor.

Table 9 shows the frequency of sensor pairings by each beacon across the first 24 measurement cycles, categorized by how many sensor positions the identified sensor deviated from the correct one. Specifically, the table details how often each beacon correctly identified the sensor directly facing it (0 deviation), as well as how often the beacon selected a sensor that was one position away (-1 for counterclockwise or 1 for clockwise) or two positions away (-2 for counterclockwise or 2 for clockwise). The subsequent Table 10 summarizes these findings, presenting the overall accuracy of the sensor connections for Run 1 in terms of correct connections, and those that were one or two positions away from the correct sensor. These tables reveal that while a majority of the sensor pairings were correct, a significant proportion deviated by one sensor position, with a smaller percentage deviating by two

| Timestamp Measurement | Tag sensor paired with Beacon 1 | | Tag sensor paired with Beacon 2 | | Tag sensor paired with Beacon 3 | |
|---|---|---|---|---|---|---|
| | Used | Actual | Used | Actual | Used | Actual |
| 0 | 5 | 0 | 2 | 2 | 4 | 4 |
| 0.619168997 | 5 | 5 | 2 | 2 | 3 | 3 |
| 1.238169193 | 5 | 5 | 1 | 1 | 3 | 3 |
| 1.857315302 | 0 | 4 | 1 | 1 | 3 | 3 |
| 2.476186037 | 4 | 4 | 1 | 1 | 2 | 3 |
| 3.095070839 | 4 | 4 | 1 | 0 | 2 | 2 |
| 3.713696003 | 4 | 4 | 5 | 0 | 3 | 2 |
| 4.332721233 | 3 | 3 | 0 | 5 | 2 | 2 |
| 4.951426983 | 3 | 3 | 0 | 5 | 1 | 1 |
| 5.570312977 | 2 | 3 | 0 | 4 | 1 | 1 |
| 6.19025588 | 3 | 2 | 4 | 4 | 1 | 0 |
| 6.808872938 | 2 | 2 | 4 | 4 | 0 | 0 |
| 7.427464485 | 2 | 2 | 4 | 3 | 0 | 5 |
| 8.046838045 | 1 | 2 | 3 | 3 | 0 | 5 |
| 8.66537714 | 2 | 1 | 3 | 3 | 5 | 5 |
| 9.284485102 | 1 | 1 | 3 | 3 | 4 | 4 |
| 9.90341115 | 1 | 0 | 2 | 2 | 4 | 4 |
| 10.52206564 | 0 | 0 | 2 | 2 | 4 | 4 |
| 11.14111376 | 0 | 5 | 2 | 2 | 3 | 3 |
| 11.75994945 | 0 | 5 | 1 | 1 | 3 | 3 |
| 12.37889385 | 4 | 4 | 1 | 1 | 3 | 3 |
| 12.99795556 | 4 | 4 | 1 | 1 | 2 | 3 |
| 13.61696196 | 4 | 4 | 1 | 0 | 2 | 2 |
| 14.235744 | 4 | 4 | 0 | 0 | 2 | 2 |
| 14.85283279 | 4 | 3 | 0 | 5 | 1 | 2 |

Figure 34: Pairings between each beacon and tag sensor. Green is facing the closest sensor, yellow a sensor next to the closest sensor, red a different sensor.

Table 9: Deviation of Sensor Identification for Each Beacon

| difference | -2 | -1 | 0 | 1 | 2 |
|---|---|---|---|---|---|
| Beacon 1 | 0 | 20 | 58 | 16 | 3 |
| Beacon 2 | 1 | 11 | 67 | 16 | 2 |
| Beacon 3 | 0 | 11 | 76 | 9 | 1 |
| Total | 1 | 42 | 201 | 41 | 6 |

Table 10: Accuracy of sensor connections for Run 1

| Metric | Correct Connections (%) | One Sensor Away (%) | Two Sensors Away (%) |
|---|---|---|---|
| Run 1 | 69.07 | 28.52 | 2.41 |

positions. This pattern suggests that the sensors might have a broader field of detection than initially expected, as the "incorrect" pairings still produced location data close to the actual positions.

# 6 Conclusions

The goal of this research was to enhance the RTLS based on ultrasound developed by Bas van Aalst. The first test focused on sensor accuracy using the direct method, which yielded satisfactory results. We explored the sensors' ability to maintain distance measurements while objects passed through; however, many materials lacked the necessary properties for these sensors to do so. When the sensors were connected to different microcontroller boards, synchronization issues arose. This was resolved by averaging the results from the sensor pairs, which provided an accuracy comparable to the setup when both sensors were connected to the same microcontroller.

The system was extended with an automated setup phase for beacon positioning, improving deployment speed and reducing human error, thus increasing overall system accuracy. Object tracking capabilities were tested, resulting in an average error of 7.65 cm per measurement. This error could be reduced further by addressing the bias caused by points too close to the base beacon. During testing, the connection between the beacons and the tag was maintained 100% of the time, indicating a strong reliability. Finally, the orientation of the moving tag was tested, and we found that the sensors received signals from a wider angle than expected, requiring further adjustments to achieve full maturity of this feature.

## 6.1 Further Research

In future extensions, these beacons can be designed such that they can send and receive signals in all directions, or can operate on different sound frequencies to reduce signal interference and improve accuracy. This will improve the flexibility and scalability of the system, making it suitable for various applications.

Additionally, the scalability of the system can be enhanced due to the capabilities of the direct method, which allows signals to travel much further than in the reflective method. This reduces the need for a large number of beacons to cover a wide area. However, if additional coverage is still required, a possible solution would be to arrange the beacons so that they form a network of triangles across the area. Each group of three beacons would create a perfect triangle, and subsequent sets of beacons would form additional non-overlapping triangles. This structured approach would ensure efficient and complete coverage.

# References


[Ali22] Fuad Aliew. An approach for precise distance measuring using ultrasonic sensors. *Engineering Proceedings*, 24(1), 2022.

[AM22] Safar M. Asaad and Halgurd S Maghdid. A comprehensive review of indoor/outdoor localization solutions in iot era: Research challenges and future perspectives. *Comput. Netw.*, 212(C), jul 2022.

[AMTF+11] L. Alonso, V. Milanés, C. Torre-Ferrero, J. Godoy, J. P. Oria, and T. de Pedro. Ultrasonic sensors in urban traffic driving-aid systems. *Sensors (Basel, Switzerland)*, 11(1):661–673, 2011.

[BW99] H.G. Berns and R.J. Wilkes. Gps time synchronization system for k2k. In *1999 IEEE Conference on Real-Time Computer Applications in Nuclear Particle and Plasma Physics. 11th IEEE NPSS Real Time Conference. Conference Record (Cat. No.99EX295)*, pages 480–483, Santa Fe, NM, USA, May 1999. IEEE.

[DDM20] Dr. Christopher Leskiw, Dr. Guojiang Gao, and Matthew Lowe. ZeroKey's Quantum RTLS Indoor Positioning System. White Paper, April 2020.

[LAY19] Qiongzheng Lin, Zhenlin An, and Lei Yang. Rebooting ultrasonic positioning systems for ultrasound-incapable smart devices. In *The 25th Annual International Conference on Mobile Computing and Networking*, MobiCom '19, New York, NY, USA, 2019. Association for Computing Machinery.

[MKKB10] M. MacGregor, L. Kelliher, and J. Kirk-Bayley. The physics of ultrasound - part 1. ANAESTHESIA TUTORIAL OF THE WEEK, 2010.

[MMES+20] Roberto Martinez-Maldonado, Vanessa Echeverria, Jurgen Schulte, Antonette Shibani, Katerina Mangaroska, and Simon Buckingham Shum. Moodoo: Indoor positioning analytics for characterising classroom teaching. International Society of the Learning Sciences, 2020. Best Paper Award.

[OCVM21] Kanji Ono, Hideo Cho, Hartmut Vallen, and Robert T. M'Closkey. Transmission sensitivities of contact ultrasonic transducers and their applications. *Sensors*, 21(13), 2021.

[Ope16a] OpenStax. *University Physics I: Mechanics, Sound, Oscillations, & Waves*, chapter 17.3, page N/A. OpenStax, 1st edition, 2016. Chapter 17.3: Speed of Sound, CC BY 4.0 License.

[Ope16b] OpenStax. *University Physics I: Mechanics, Sound, Oscillations, & Waves*, chapter 17.7, page N/A. OpenStax, 1st edition, 2016. Chapter 17.7: Ultrasound, CC BY 4.0 License.

[PN11] J. Prasad and C. G. Krishnadas Nair. Non-destructive test and evaluation of materials. 2011. Chapter Ultrasonics.

[QL17] Jun Qi and Guo-Ping Liu. A robust high-accuracy ultrasound indoor positioning system based on a wireless sensor network. *Sensors*, 17(11), 2017.

[RBK11] Armin Runge, Marcel Baunach, and Reiner Kolla. Precise self-calibration of ultrasound based indoor localization systems. In *2011 International Conference on Indoor Positioning and Indoor Navigation*, pages 1–8, Guimaraes, Portugal, September 2011. IEEE.

[SBBD12] Mohamed Saad, Chris Bleakley, Tarig Ballal, and Simon Dobson. High-accuracy reference-free ultrasonic location estimation. *IEEE Transactions on Instrumentation and Measurement*, 61:1561–1570, 06 2012.

[SNM20] Sittichai Sukreep, Chakarida Nukoolkit, and Pornchai Mongkolnam. Indoor position detection using smartwatch and beacons. *Sensors and Materials*, 32(2):455–473, 2020. S & M 2114.

[SS18] Anirban Sarkar and Sadia Sultana. Study on ultra-wideband (uwb) system and its applications. *Journal of Bangladesh Electronics*, 18(1–3):47–53, 2018.

[TKL12] Benjamin Thiel, Kamil Kloch, and Paul Lukowicz. Sound-based proximity detection with mobile phones. In *Proceedings of the*

*Third International Workshop on Sensing Applications on Mobile Phones*. Association for Computing Machinery, 2012.

[Unk1] Unknown. Hc-sr04 ultrasonic sensor module user guide. User Guide: Ultrasonic Sensor V2.0, 1.

[vA23] B. van Aalst. Ultrasound indoor positioning system for localisation of a moving object. Bachelor's thesis, August 2023.